A Transient Initiator for Polypeptoids Postpolymerization alpha-Functionalization via Activation of a Thioester Group

Borova, Solomiia

2022-02

Borova , S , Schlutt , C , Nickel , J & Luxenhofer , R 2022 , ' A Transient Initiator for Polypeptoids Postpolymerization alpha-Functionalization via Activation of a Thioester Group ' , Macromolecular Chemistry and Physics , vol. 223 , no. 3 , 2100331 . https://doi.org/10.1002/macp.202100331

http://hdl.handle.net/10138/341939
https://doi.org/10.1002/macp.202100331

Macromolecular Chemistry and Physics
www.mcp-journal.de

A Transient Initiator for Polypeptoids Postpolymerization α-Functionalization via Activation of a Thioester Group

*Solomiia Borova, Christine Schlutt, Joachim Nickel, and Robert Luxenhofer**

Here, a postpolymerization modification method for an α-terminal functionalized poly-(*N*-methyl-glycine), also known as polysarcosine, is introduced. 4-(Methylthio)phenyl piperidine-4-carboxylate as an initiator for the ring-opening polymerization of *N*-methyl-glycine-*N*-carboxyanhydride followed by oxidation of the thioester group to yield an α-terminal reactive 4-(methylsulfonyl)phenyl piperidine-4-carboxylate polymer is utilized. This represents an activated carboxylic acid terminus, allowing straightforward modification with nucleophiles under mild reaction conditions and provides the possibility to introduce a wide variety of nucleophiles as exemplified using small molecules, fluorescent dyes, and model proteins. The new initiator yielded polymers with well-defined molar mass, low dispersity, and high end-group fidelity, as observed by gel permeation chromatography, nuclear magnetic resonance spectroscopy, and matrix-assisted laser desorption/ionization time-of-flight mass spectroscopy. The introduced method can be of great interest for bioconjugation, but requires optimization, especially for protein conjugation.

1. Introduction

Functional polymers find broad application in the biomedical field. Inter alia, research and application in drug, protein, and gene delivery systems[1–18] self-assembled polymers,[19–23] nanoreactors,[24,25] bioimaging contrast agent carriers,[26] antibiofouling coatings,[13,27–29] sensors,[30,31] tissue engineering[32–34] requires specifically designed polymers with suitable functionalities for appropriate bioconjugation and further biomedical application.[35–37] Among the plethora of synthetic polymers, poly(ethylene glycol) (PEG) remains the commercially available "gold standard" for biomedical application due to its high hydrophilicity combined with good solubility in organic solvents,[38] low toxicity,[39] and stealth behavior.[40] In addition, structural varieties such as star-PEG and a considerable diversity of end-group functionalization[38,41–43] are commercially available. Despite PEG being generally regarded safe, antibodies against PEG[44–47] and some other limitations such as toxic side products,[48,49] hypersensitivity,[50,51] vacuolization,[52–54] and accumulation in the body[40,54,55] were reported. Several studies reported on already pre-existing antibodies in several patients[56,57] during clinical trials with PEGylated therapeutic agents. Hamad et al. demonstrated that depending on PEG concentration and molar mass, unexpected anaphylaxis in some sensitive individual animals could occur[58] after administration with medicines containing a high concentration of PEGylated carriers. Zhang[59] and later Zhao et al.[60] reported on the toxic influence of PEG-modified particles. Accordingly, the search for alternatives has been a going research topic in the chemistry community. Especially, safe alternatives are again of particular interest in the current COVID-19 pandemic considering the allergic reaction and/or anaphylaxis after vaccination with currently developed vaccines.[61,62] These side effects have been associated with any of the vaccine components, including PEG and PEG derivatives.[62,63] Among some other polypeptides, polypeptoids, and poly(2-oxazoline)s, have been suggested as excellent candidates to substitute PEG.[23,64–67]

Polypeptides and polypeptoids have had significant attention for biomedical application for decades and saw an additional boost in the last few years.[68–72] The absence of hydrogen bonds[73,74] in polypeptoids gives them potential advantages, such as better solubility in various solvents and will form random coils instead of secondary structures often observed for polypeptides. However, formation of relatively stable helices or sheet structures have been reported for specific side chains that favor specific conformations.[68,75,76]

S. Borova, C. Schlutt, R. Luxenhofer
Functional Polymer Materials, Chair for Advanced Materials Synthesis, Institute for Functional Materials and Biofabrication, Department of Chemistry and Pharmacy
Julius-Maximilans-University of Würzburg
Röntgenring 11, Würzburg, Bavaria 97070, Germany
E-mail: robert.luxenhofer@uni-wuerzburg.de
J. Nickel
Department of Tissue Engineering and Regenerative Medicine
University Hospital of Würzburg
Röntgenring 11, Würzburg, Bavaria 97070, Germany
R. Luxenhofer
Soft Matter Chemistry, Department of Chemistry and Helsinki Institute of Sustainability Science, Faculty of Science
University of Helsinki
P.O. Box 55, Helsinki 00014, Finland

The ORCID identification number(s) for the author(s) of this article can be found under https://doi.org/10.1002/macp.202100331

DOI: 10.1002/macp.202100331

Hydrophilic polysarcosine (PSar)[23,72] and somewhat lesser hydrophilic poly(*N*-ethyl-glycine) (PNEG)[77,78] could be potentially used in the biomedical field as water-soluble polymers. PSar due to nontoxicity,[68,79,80] biocompatibility,[64,81] nonfouling,[82–84] low (or no) cytotoxicity,[68,72,80,85] electroneutrality[86] is considered as promising alternative to PEG.[10,87]

PSar is most commonly prepared via nucleophilic living ring-opening polymerization (NuLROP) of *N*-substituted *α*-amino acid-*N*-carboxyanhydrides (NNCAs),[88,89] which can be initiated with a variety of nucleophiles. Most commonly, amines are employed,[90–92] but water,[92] alcohol,[93–95] thiols,[96] and others[70,92,97–100] have been reported. Notably, PSar and other polypeptoids can also be obtained by NuLROP from the more stable *N*-substituted *α*-amino acid-*N*-thiocarboxyanhydrides (NNTAs).[101,102] Apart from determining the polymer chain length via $[M]_0/[I]_0$, an initiator can be chosen to introduce specific functional groups in the *α*-terminus of the polymers. However, it is important to consider that the introduced functionalities must be compatible with the polymerization process. Only a few papers introduced functional initiators for NCAs polymerization. Tao et al. reported on ROP of *N*-substituted glycine *N*-thiocarboxyanhydride with cysteamine with a further application for thiol-ene and thiol-yne click chemistry.[103] Later, Johann and co-workers introduced the amino-functional *trans*-cyclooctenes (TCO) and 6-methyl-tetrazine (mTz) as initiators to obtain functional polypeptoids and performed their postpolymerization modification.[104] Postpolymerization modification (PPM) can help to overcome limitations that occur during polymerization and introduce responsive, structural, and functional properties into polymers, which are otherwise incompatible with the polymerization process.[36,105–108] PPM can offer several advantages. On one hand, a variety of different functionalities can be introduced into the side chain or termini of a polymer. On the other hand, the resulting polymer will have the same degree of polymerization and chain length distribution as the original polymer. PPM also allows the synthesis of polymers with functionalities that cannot or only inconveniently be introduced directly via the polymerization.

Different postpolymerization concepts like modification of polymeric active esters, anhydride, isocyanates, oxazolones, epoxides, Michael-type addition reactions, modification by thiol exchange, etc., have been reported for functionalization of polymers.[36] PPM used for bioconjugation, in particular, should offer high efficacy under mild conditions. In the last two decades, click-chemistries have had a major impact in the field of bioconjugation.[109] Despite the preference for PPM utilizing click chemistry, the activated ester exchange reaction still has some value.

The PPM via polymeric active esters became an attractive tool after the first introduction by Jatzkewitz[110–112] and later picked up by Ferruti et al.[113] and Ringsdorf et al.[114] The reaction of activated esters with amines leads to the formation of stable amide bonds which are of course most common in biological systems. Additionally, there is no need to use of potentially toxic (metal) catalysts or other chemical reagents making them an attractive material in biomedical research.[115] Apart from alkyne-azide click chemistry,[116–121] sulfur-based chemistries have been widely exploited.[122–126] Thiol moieties exhibit a favorable low pK_a,[127,128] have ability to form disulfide bonds upon oxidation,[129,130] show a good reactivity profile[131] and are abundant in biological systems.[132] The versatility of sulfur-based chemistry and the ease of modification makes it an attractive choice in organic chemistry and life science.[133–135] A multitude of chemoselective reactions utilizes sulfur chemistry[135–138] with application in many fields, including self-healing materials or drug delivery systems.[122,139] One particular thiol-based reagent, 4-(methylthio)phenol (4MTP), has been described long ago for peptide coupling, but to date, has not been investigated for PPM bioconjugation. Johnson et al. reported on the use of 4MTP esters as a carboxy-protecting group during polypeptide synthesis in 1968. When 4MTP is oxidized to yield 4-(methylsulfonyl)phenyl ($4MTO_2P$), it transforms a protected ester into an activated ester, allowing further aminolysis and amide formation.[140–142] Chen introduced 4MTP esters for quinoxaline antibiotic synthesis.[143] Later, Siemens applied activated 4MTP esters during peptide solid-phase synthesis.[144] Cho also reported on the application of 4MTP moieties as a safety-catch protecting group during peptide coupling or as an active ester that can act with other N-free peptide fragments to form new bonds.[145] More recently, Popovic' et al. reported on peptide 4MTP ester synthesis suitable for peptide segment coupling or direct amidation with peptide *N*-termini.[146] However, to the best of our knowledge, 4MTP has not been utilized or suggested for any PPMs.

Here, we introduce 4-(methylthio)phenyl piperidine-4-carboxylate (4MTPPC) as a novel functional initiator for the NuLROP of NCAs, in particular *N*-phenyloxycarbonylsarcosine (Poc-Sar), which forms Sar-NCA in situ.[147,148] The oxidation of the 4MTPPC into a $4MTO_2PPC$ transforms the protected carboxylic acid into an activated acid, which then readily reacts with nucleophiles (**Figure 1**). Accordingly, we introduce a novel bioconjugation strategy for polypeptoids which could be also utilized in polypeptides and potentially, after some adjustments, for other polymers. Although it appears that the presented approach is not as efficient as typical click-chemistry, its simplicity and straightforward incorporation into many standard bioconjugation strategies and due to its orthogonality with many click-chemistry approaches, it is a valuable supplement to the bioconjugation toolbox.

2. Experimental Section

2.1. Materials and Methods

2.1.1. Materials

Dichloromethane (DCM), *N*, *N*-dimethylformamide (DMF), *N*-methyl morpholine (NMP), 1-(tert-butoxycarbonyl)piperidine-4-carboxylic acid (Boc-Inp-OH), trifluoroacetic acid (TFA), 4-(dimethylamino)-pyridine (DMAP), diphenylcarbonate (DPC), 3-chloroperoxybenzoic acid (*m*-CPBA), hexane, ethyl acetate (EtOAc), ethanol (EtOH), 4-(methylthio)phenol (4MTP), sarcosine (Sar) were purchased from Sigma-Aldrich or TCI and used without further purification. DCM was dried over $CaCl_2$ before further use. Triethylamine (TEA) was dried over BaO and distilled before use.

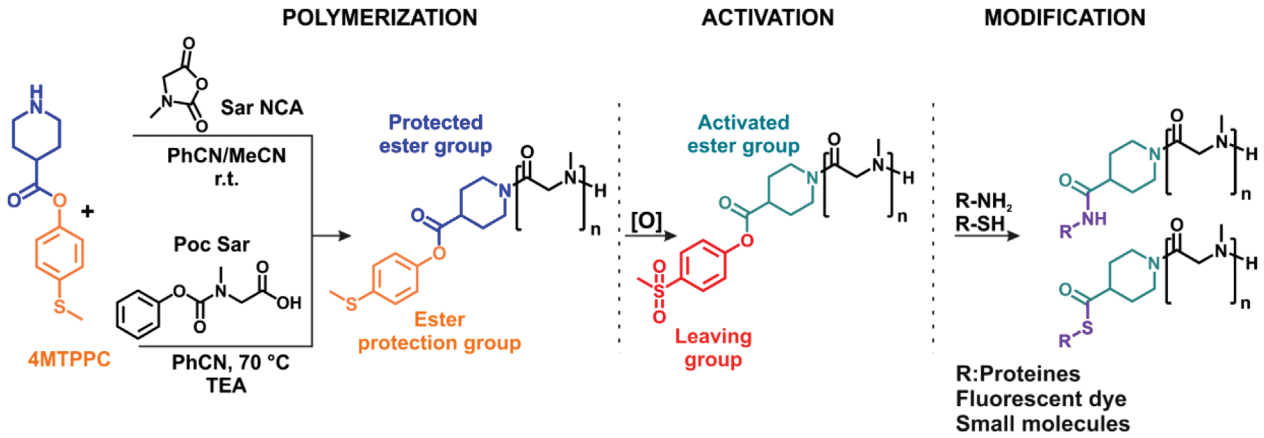

Figure 1. Postpolymerization modification concept based on ring-opening polymerization of *N*-phenoxycarbonyl-*N*-methylglycine (Poc Sar) and/or *N*-methylglycine-*N*-carboxyanhydride (Sar NCA) with 4-(methylthio)phenyl piperidine-4-carboxylate (4MTPPC) initiator via activation of 4-(methylthio)phenol (4MTP) ester group.

2.1.2. Methods

NMR spectra were recorded on a Fourier 300 (^{1}H; 300.12 MHz), Bruker Biospin (Rheinstetten, Germany) at 298 K. The spectra were calibrated to the signal of residual protonated solvent ($CDCl_3$: 7.26 ppm, D_2O: 4.79 ppm, CD_3CN: 1.94 ppm, $(CD_3)_2SO$: 2.50 ppm).

Gel permeation chromatography (GPC) was performed on a Polymer Standard Service (PSS, Mainz, Germany) system (pump mod. 1260 infinity, RI-detector mod. 1260 infinity, precolumn GRAM 10×10^{-6} M (50×8 mm)), with HFIP (containing 3 g L^{-1} potassium trifluoroacetate (KTFA)) as eluent and calibrated against PEG standards with molar mass ranging from 106 g mol^{-1} to 100 kg mol^{-1}. Columns were kept at 40 °C and the flow rate was set to 0.7 mL min^{-1}. Data were processed using WinGPC Unichrom V.8.20 Build 5350 software. Before each measurement, samples were filtered through 0.2 µm PTFE filters (Rotilabo, Karlsruhe).

Matrix-assisted laser desorption/ionization time-of-flight (MALDI-ToF) mass spectra were recorded on a Daltonics autoflex II LRF 50 or a Daltonics UltrafleXtreme (Bruker, Bremen, Germany) using an N_2 laser (λ = 337 nm). All spectra were recorded in positive reflector mode. Detection was typically set from 1000 to 7000 m z^{-1}. After parameter optimization, the instrument was calibrated with CsI_3 or PEG standards depending on the m/z range of the individual sample. Samples were prepared with α-cyano-4-hydroxycinnamic acid or with sinapinic acid as matrices, using the dried-droplet spotting technique (0.5–1.5 µL). Exemplarily, samples (1 g L^{-1}) were dissolved in MeOH (supplemented with 1.0% TFA) or in MeCN. Laser power was set slightly above the threshold, typically at 50–70%. Poisson distributions for comparision with experimental mass spectra were calculated using Equation (1)

$$P(DP)(X = k) = \frac{DP^k}{k!} e^{(-DP)} \quad (1)$$

The M_n, M_w were calculated using Equation (2) from peak analysis obtained from MALDI-ToF experimental data

$$M_n = \frac{\Sigma N_i M_i}{\Sigma N_i} \quad M_w = \frac{\Sigma N_i M_i^2}{\Sigma N_i M_i} \quad (2)$$

where N_i and M_i are the intensity and mass of the *i*-th polymer, respectively.

Ultraviolet–visible (UV–Vis) spectrum was taken on a Jasco V-630 spectrometer in MeOH in a quartz cuvette (0.1 or 1.0 cm). The concentration of the dye was calculated by UV–vis spectroscopy in an absorption maximum of 325 nm.

The polymers were purified via dialysis. Dialysis was performed using Spectra/Por membranes with a molecular weight cutoff (MWCO) of 1 and 10 kDa (material: cellulose acetate) obtained from *neoLab* (Heidelberg, Germany) against water (Millipore).

RFP conjugated polymers were purified via centrifugal filters (Amicron Ultra-15) with a membrane MWCO of 10 kDa (material: regenerated cellulose) obtained from Millipore (Germany). 1 mL (concentration: 1g/L) of the conjugated sample was placed in to filtration device and centrifuged twice at 14 000 rpm for 15 min.

Fast protein liquid chromatography (FPLC) was carried out on an Äktaavant (GE Healthcare, Chalfont St. Giles, Great Britain) to analyze resulting PSar conjugates. A GL 10/300 Column (300 mm, Ø 10 mm, GE Healthcare) was packed with Superdex 75 resin under constant pressure. The purification was conducted in 10×10^{-3} M TRIS buffer with 300×10^{-3} M of NaCl (pH = 8.0) with a linear flow of 0.5 mL min^{-1}.

Sodium dodecyl sulfate–polyacrylamide gel electrophoresis (SDS-PAGE) was used to analyze protein-polymer conjugates on 12% PAGE under nonreducing conditions, using standard molecular biology technique. After electrophoresis gels were stained using Coomassie brilliant blue R250. In case of RFP

conjugates fluorescent bands were detected using a FluorChem Q imaging system (Biozym).

2.2. Synthetic Procedures

2.2.1. Monomer Synthesis – Sarcosine NCA

The Sarcosine NCA was synthesized as was described previously.[149] Sarcosine 5.00 g (0.056 mol, 1.7 eq.) predried by azeotropic distillation with toluene was placed in 250 mL dried Schlenk flask and suspended in 90 mL of dry THF under a steady flow of argon followed by the addition of 4.0 mL (0.033 mol, 1.0 eq.) diphosgene via syringe. The continuous flow of argon was turned off, and the reaction mixture was heated to 66 °C. The reaction vessel was equipped with a washing bottle containing 35 wt% potassium hydroxide (KOH) solution to neutralize the developing HCl. Stirring and heating were continued until all solid was dissolved, and the dark brown solution was obtained (around 3.0 h). The solvent was evaporated under reduced pressure, yielding a brownish oil as a crude product. 5.0 mL of dry petrol ether was added to the obtained product under a steady argon flow and left in the fridge overnight to solidify. The solid was decanted under an argon atmosphere, dried under reduced pressure, and subsequently sublimated *in vacuo* (4.00 g, 80%).

^{1}H NMR (300 MHz; $CDCl_3$): δ = 3.04 ppm (3 H, s, CH_3–), 4.12 ppm (2 H, s, –CH_2–CO–)

2.2.2. Synthetic of Poc-Sar

The synthesis procedure was performed as follows.[148] Sarcosine 50 g (0.56 mol, 1.0 eq.) was suspended in 500 mL of MeOH. KOH (31.5 g, 0.56 mol, 1.0 eq.) and 23.7 g (0.56 mol, 1.0 eq.) LiCl was dissolved in 300 mL of MeOH and added to a sarcosine suspension. Diphenylcarbonate (DPC) 120 g (0.56 mol, 1.0 eq.) was dissolved in 200 mL of THF, and the rest of the DPC was washed with an additional 200 mL of THF. The reaction flask was left to react for 7–9 days at room temperature. Subsequently, the reaction mixture was filtered, and volatiles was removed under reduced pressure. The residue was dissolved in 400 mL of 5% $NaHCO_3$ and extracted three times with 300 mL of ethyl acetate (EtOAc). The water phase was adjusted to pH 3–4 with concentrated HCl and extracted three times with 300 mL of EtOAc. The organic phase was dried under Na_2SO_4 overnight. The solvent was removed under reduced pressure, and the high viscous gel was obtained as the raw product. The yield of the obtained product is 37.6% (44.1 g).

^{1}H NMR (300 MHz; $CDCl_3$): δ = 3.01–3.24 ppm (3 H, s, –CH_3), 4.09–4.25 ppm (2H, d, –CH_2–N–), 7.04–7.42 ppm (5 H, m, aromatic ring). ^{13}C NMR (300 MHz; $CDCl_3$): δ = 36.4 ppm (1C, N–CH_3), 50.81 ppm (1 C, CH_2–N–), 121.9 ppm (2C, phenol ring), 125.8 ppm (1C, phenol ring), 129.5 ppm (2C, phenol ring), 151.3 ppm (1C, phenol ring), 155.84 ppm (1C, N–C(O)–O–), 174.45 ppm (1C, C(O)–O–).

2.2.3. Synthesis of 4-(methylthio)phenyl piperidine-4-carboxylate (4MTPPC)

Boc-Inp-OH 2.01 g (8.75 mmol, 2.0 eq.) was dissolved in 60 mL of chloroform and treated with 1.80 g (8.75 mmol, 2.0 eq.) dicyclohexylcarbodiimide (DCC) for 15 min. Subsequently, 4MTP 0.61 g (4.37 mmol, 1 eq.) was added followed by DMAP 0.107 g (0.874 mmol 0.2 eq.) and 4-methyl morpholine 0.885 g (8.75 mmol 2 eq.). The mixture was left to react at room temperature for 5.0 h. The reaction solution was further treated with 18 mL of TFA for 30 min at room temperature to remove the Boc protecting group. The crude product was obtained by precipitating twice from cold diethyl ether and dry dried *in vacuo*. The yield of the obtained product is 93% (0.93 g).

^{1}H NMR (300 MHz, D_2O): δ = 7.42 ppm (2H, d, –CH═), 7.14 ppm (2H, d, –CH═), 3.62–3.33 ppm (2H, m, –CH_2–), 3.33–3.00 ppm (2H, m, –CH_2–), 2.53 ppm (3H, s, CH_3–S–), 2.37 ppm (2H, m, –CH_2–), 2.20–1.88 ppm (2H, m, –CH_2–). ^{13}C NMR (300 MHz; CD_3CN): δ = 15.06 ppm (1C, –S–CH_3), 24.23 ppm (2C, –CH_2– piperidine), 37.93 ppm (1 C, –CH– piperidine), 42.75 ppm (2C, –CH_2– piperidine), 127.15 ppm (2C, –CH = aromatic ring), 127.40 ppm (2C, –CH = aromatic ring), 136.1 ppm (1C, –S–C = aromatic ring), 147.97 ppm (1 C, (O)—O—C— aromatic ring), 172.98 ppm (1C, —O—C(O)).

2.2.4. Synthesis of PSar

The synthesis of PSar was adapted from literature[92] and.[94,95]

2.2.5. Polymerization of Sar-NCA

The monomer solution was prepared in a dried Schlenk flask under an inert atmosphere by dissolving Sar-NCA 1.47 g (13.03 mmol, 96.5 eq.) and 4MTPPC 0.034 g (0.135 mmol, 1.0 eq) in 5 mL of benzonitrile (PhCN) and 3 mL of acetonitrile (MeCN). The reaction solution was stirred under an inert and dry atmosphere at room temperature for 24 h. In the first 2.0 h, a vial was opened to reduce CO_2. PSar was purified by precipitation (3x) from cold diethyl ether (redissolved in DCM) and lyophilized.

2.2.6. Polymerization of Sar-NCA from Poc-Sar

The same procedure was performed with Poc-Sar. Poc-Sar 0.6 g (2.87 mmol, 50 eq.) and 4MTPPC 0.0185 g (0.074 mmol, 1.0 eq.) was dissolved in 4 mL of PhCN and 2 mL of MeCN. After the initiator and monomer were dissolved, 0.4 mL (0.29 g 2.87 mmol, 50 eq.) of TEA was added, and the reaction solution was heated up to 70 °C and left to react for 24 h. The pure polymer was obtained by precipitation (3x) from cold diethyl ether (redissolved in DCM) and lyophilized.

2.2.7. Oxidation of PSar

The oxidation of PSar was performed according to the procedure described by Gradisar et al.[96] PSar 0.142 g (0.0596 mmol, 1.0 eq.) was dissolved in 5 mL dry DCM and cooled to 0 °C in an ice bath. m-CPBA 0.021 g (0.119 mmol, 2.0 eq.) was dissolved in 3 mL DCM, added dropwise to the polymer solution and stirred for 3–5 h, while warming to room temperature. The resulting polymer was twice precipitated from cold diethyl ether and dried under vacuum with the following dissolution in water and lyophilization to give the white powder (0.128 g, 89%).

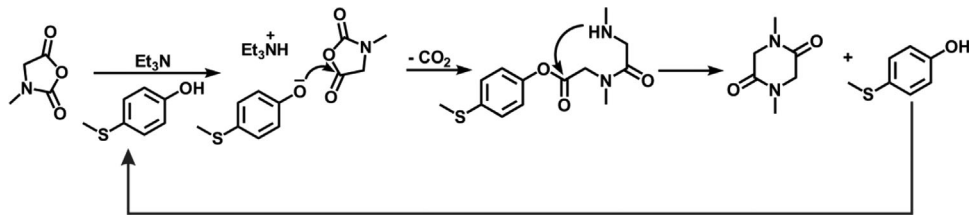

Figure 2. Hypothetic mechanism illustration the formation of cyclic dimers during polymerization with 4(methylthio)phenol.

^{1}H NMR (300 MHz, $CDCl_3$): δ = 7.99 ppm (2H, d, –CH═), 7.32 ppm (2H, d, –CH═), 3.62–3.33 ppm (2H, m, $-CH_2-$), 3.33–3.00 ppm (2H, m, $-CH_2-$), 3.07 ppm (3H, s, CH_3-SO_2-), 2.37 ppm (2H, m, $-CH_2-$), 2.20–1.88 ppm (2H, m, $-CH_2-$).

2.2.8. Functionalization of PSar

A substitution was performed as follows. Oxidized PSar was dissolved in 5 mL DCM (or any other suitable solvent) and stirred with 3.0 eq. of nucleophile overnight. The products were obtained by precipitation from cold diethyl ether followed by dialysis and lyophilization.

3. Results and Discussion

This work presents a synthetic pathway to obtain 4MTPPC-functionalized polypeptoids via NuLROP using a new 4MTP-functionalized initiator. As was already mentioned, the presence of a 4MTP group in the α-position of the polymer should allow the subsequent introduction of diverse functionalities via post-polymerization nucleophilic substitution.

Previous work by Chan et al. suggests that it is possible to initiate ROP of NCAs or NNCAs with alcohols.[94] In their contribution, *N*-butylglycine *N*-carboxyanhydride was employed as a monomer. However, the authors found that phenol proved challenging for this purpose. Nevertheless, we investigated 4-(methylthio)phenol (4MTP) to initiate the ROP of Sar-NCA and Poc-Sar. In line with the results by Chan et al., this approach proved not satisfactory. PSar obtained from Poc-Sar and initiated with 4MTP in PhCN had a much higher molar mass than expected from $[M]_0/[I]_0$ (16.2 vs 3.7 kg mol^{-1}) and a broad molar mass distribution ($Đ$ = 2.03). The molar mass of polymers obtained from Sar-NCA and 4MTP was also too high, and GPC traces were bimodal. These issues may be attributed to poor initiation efficiency and/or slow initiation. Chan et al. suggested that adjusting the type of alcohol, solvent and base can lead to more satisfactory results, however, our strategy relies on the 4MTP moiety. Also, polymerization in $CHCl_3$ or MeCN did not show significant improvement. The molar masses of the obtained PSar remain higher than expected (5.1, 5.0, and 2.1 vs 1.6 kg mol^{-1}). The dependence of the reaction rate on the nature of the solvent was characterized by NMR spectroscopy. ^{1}H NMR analysis shows presence of significant amounts of diketopiperazine dimer (12% in MeCN, 27% in PhCN, and 35% in $CHCl_3$, respectively, of total Sar units) formed during the polymerization (Figure S1, Supporting Information). The presence of such large amount of dimer suggests that the propagating amine is capable of attacking the ester group in the α-position of the polymer chain end and forming a diketopiperazine dimer or, potentially higher molar mass cyclic polypeptoids (**Figure 2**). The nature of solvent has apparently a significant influence on the polymerization behavior, as evidenced by the different amounts of formed diketopiperazine dimers found in the investigated solvents. In $CHCl_3$, monomer consumption was fastest and a markedly higher proportion of cyclic dimer was observed compared to the reactions carried out in MeCN and PhCN. Signals that can be attributed to 4MTP-initiated PSar were observed in ^{1}H NMR spectra (Figure S2, Supporting Information). Signals that can be assigned to free 4MTP are also observed. In contrast, no aromatic signals are detected after polymerization in MeCN. As control, we performed the initiation of Sar NCA polymerization with 4MTP with and without TEA. In both cases, the M_n of the resulting PSar is much higher than expected. The ^{1}H NMR spectra showed the presence of the free 4MTP when TEA was not utilized (Figure S3, Supporting Information). Based on obtained results, we considered that mostly 4MTP initiated ROP of Sar NCA. However, recently, Gebru et al. reported on the influence of the TEA concentration on the control over ROP of Sar NCA using dopamine hydrochloride as an initiator.[150] The authors claimed that the polymerization is not well controlled at a higher TEA ratio, and the used base could mask the activity of the catechol moieties. In addition, traces of water would protonate TEA leading to the formation of hydroxyl anions which could also initiate the ROP. In any case, the initiation using 4MTP and results in poor initiation efficiency and control, and higher M_n than desired. MALDI-ToF mass spectrometry of the product obtained from $CHCl_3$ confirmed low molar mass. Unfortunately, the desired product (MTP-initiated PSar) and the macrocyclic PSar have a very similar m/z ratio and isotope pattern, and therefore we cannot easily distinguish the two by mass spectrometry (Figures S4 and S5, Supporting Information). The signal attributed to PSar initiated with 4MTP was observed. However, the presence of low molecular weights cyclic polypeptoids or dimers could not be determined. Interestingly, the obtained signals could also be assigned to oxidized or partly oxidized PSar initiated with 4MTP even though no oxidation was performed. In addition, MALDI-ToF MS data corroborate the molar mass values obtained by GPC (Figure S1, Supporting Information).

In summary, 4MTP can initiaton PSar polymerization, but control is poor. Therefore, we investigated a different strategy, i.e., synthesis of an initiator that contains 4MTP but initiates the ROP through a more reliable nitrogen nucleophile (**Figure 3**a) and prevents dimer formation at the same time.

While commonly secondary amines are not considered good nucleophiles (they are more basic than nucleophilic in character), piperidine and its derivatives are good nucleophiles due to the cyclic constraint.

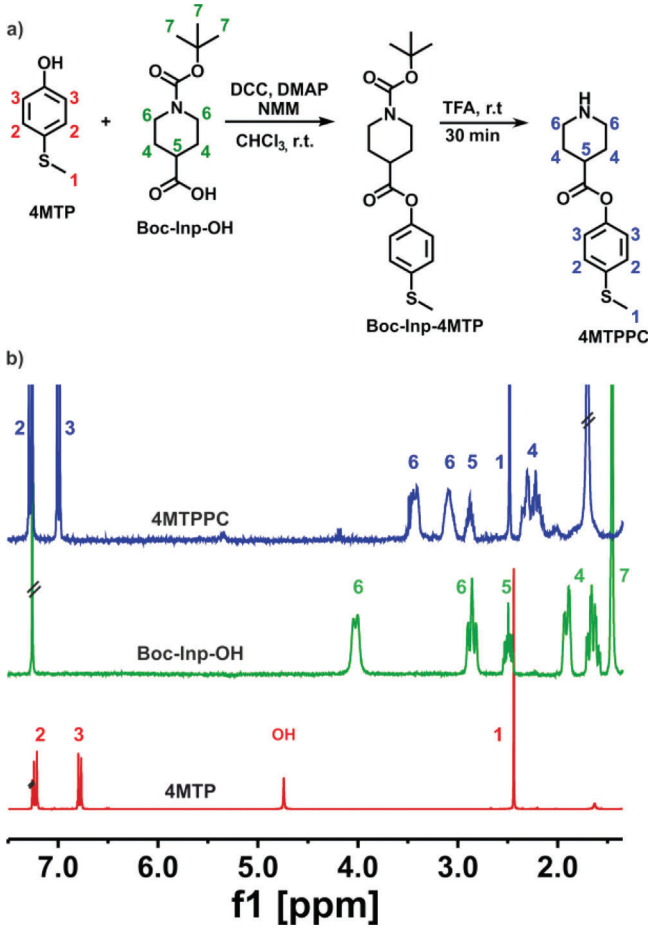

Figure 3. a) Synthetic scheme for the preparation of 4-(methylthio)phenyl piperidine-4-carboxylate (4MTPPC) by esterification of *N*-Boc-isonipecotic acid with 4-(methylthio)phenol. b) ^{1}H NMR (300 MHz, $CHCl_3$, 297 K) spectra of 4-(methythio)phenol (red), 1-(tert-butyloxycarbonyl)piperidine-4-carboxylic acid (green), and 4-(methylthio)phenol piperidine-4-carboxylate (blue) with respective signal assignment.

Accordingly, 4-(methylthio)phenyl piperidine-4-carboxylate (4MTPPC) was successfully synthesized in two steps. In the first step, we performed the esterification of Boc-Inp-OH with 4MTP, followed by TFA treatment to remove the Boc group in a second step (Figure 3a). The product was obtained as a white powder with a good yield (93%) and satisfactory purity. ^{1}H-NMR spectra analysis of the novel initiator in $CDCl_3$ shows the characteristic signal of the methyl group of the thioether (2.48 ppm, blue) and aromatic protons (7.29 and 7.01 ppm) of 4MTP (Figure 3b). The signal attributed to the 4MTP methyl group (signal 1, blue) is shifted slightly to higher ppm values due to the introduced ester group. Signals 4 and 6 (blue and green, respectively) are represented with two peaks that most likely arise from the axial and equatorial chair conformation of the piperidine group.[151,152]

The synthesis of PSar was performed by ROP of Sar-NCA monomer according to a well-known method.[148,149] In contrast to initiation using 4MPT initiation, this approach proved successful. NMR spectra analysis of the resulting polymers shows significant signals attributed to PSar initiated with 4MTPPC initiator. GPC traces of the obtained polymer are narrow, monomodal and are in good agreement with expected values from $[M]_0/[I]_0$ data (M_n = 2.9 vs 3.3 kg mol^{-1}). We also tested this initiator using an alternative monomer for PSar synthesis. Synthesis of Sar-NCA requires the use of toxic and harmful chemicals (phosgene or thionyl chloride). Also, the purification, handling and storage of the moisture-sensitive NCA is challenging. To address this, Yamada introduced *N*-phenyloxycarbonyl amino acids for polypeptide synthesis, which was later adopted by Doriti[147,148] for polypeptoids. Such monomers can be synthesized in high purity, good yield, and stability and polymerized to well-defined polypeptides/polypeptoids.

Accordingly, we initiated Poc-Sar polymerization using 4MTPPC in PhCN at 70 °C (**Figure 4**a). PSar homopolymers were obtained with 30–90% (unoptimized) yield. The yield of 30% was observed for low molecular weight PSar and is attributed to losses in the purification (precipitation) step. The products were analyzed with NMR spectroscopy, GPC and MALDI-ToF mass spectrometry.

^{1}H NMR spectra analysis shows the expected signals 2, 3 (at 7.41 and 7.17 ppm, respectively) and 1 (at 2.56 ppm) attributed to phenyl ring and methyl moieties of the 4MTPPC initiator (Figure 4b, top). Additionally, after extended storage (at 8 °C) of several months, smaller signals 2' (at 7.32 ppm), 3' (at 6.94 ppm), and 1' (at 2.48 ppm) are observed which can be attributed to 4MTP, apparently generated by hydrolysis in storage (Figure 4b, bottom). The GPC traces show a clear and controlled increase of the molar masses with increasing $[M]_0/[I]_0$, even though the experimental molar masses tended to be somewhat smaller than expected (**Figure 5**a). They also show that the resulting polymers are essentially monomodal and relatively narrowly distributed, resulting in low values for $Đ$ (Figure 5b; and Table S1, Supporting Information,). The elugram of PSar with $[M]_0/[I]_0$ = 10 significantly overlaps with the system peak and residual solvent. We also assume that the particularly low yield for PSar with DP = 10 is due to significant loss during work-up rather than due to problems with initiation/polymerization. Optimization of this work-up for the low-molar mass PSar was outside the scope of this contribution. Importantly, successful initiation with 4MTPPC was further confirmed by MALDI-ToF mass spectrometry. MALDI-ToF MS confirms the increase of molar mass with increasing $[M]_0/[I]_0$ and also the narrow molar mass distribution (Figure 5c). In all cases, the mass differences (Δ m/z) between individual signal distributions reflect the molar mass of the polymer repeat unit (71.2 g mol^{-1}). In contrast to GPC, the polymer obtained from a targeted $[M]_0/[I]_0$ = 10 shows a molar mass distribution reminiscent of a Poisson distribution, as expected for a living polymerization. The main molar mass distribution corresponds to protonated polymers initiated with 4MTPPC, bearing an amine terminus. However, M_n calculated from the main distribution (α) peak intensities is somewhat smaller than expected, with a maximum of the distribution at a DP of 7 (DP_{max} = 7). The alternative subdistribution β and γ can be attributed to the same polymer bearing potassium and sodium ion doping, respectively (Figure 5d). The signals attributed to PSar with a partly hydrolyzed α-end group carrying a sodium ion doping (ϵ) are observed. Additionally, signals of low intensities (m/z = 776) can be attributed to a polymer bearing an initiator that underwent fragmentation (Δm/z = 45), presumably during the MALDI ToF MS analysis with hydrogen ion doping (δ).

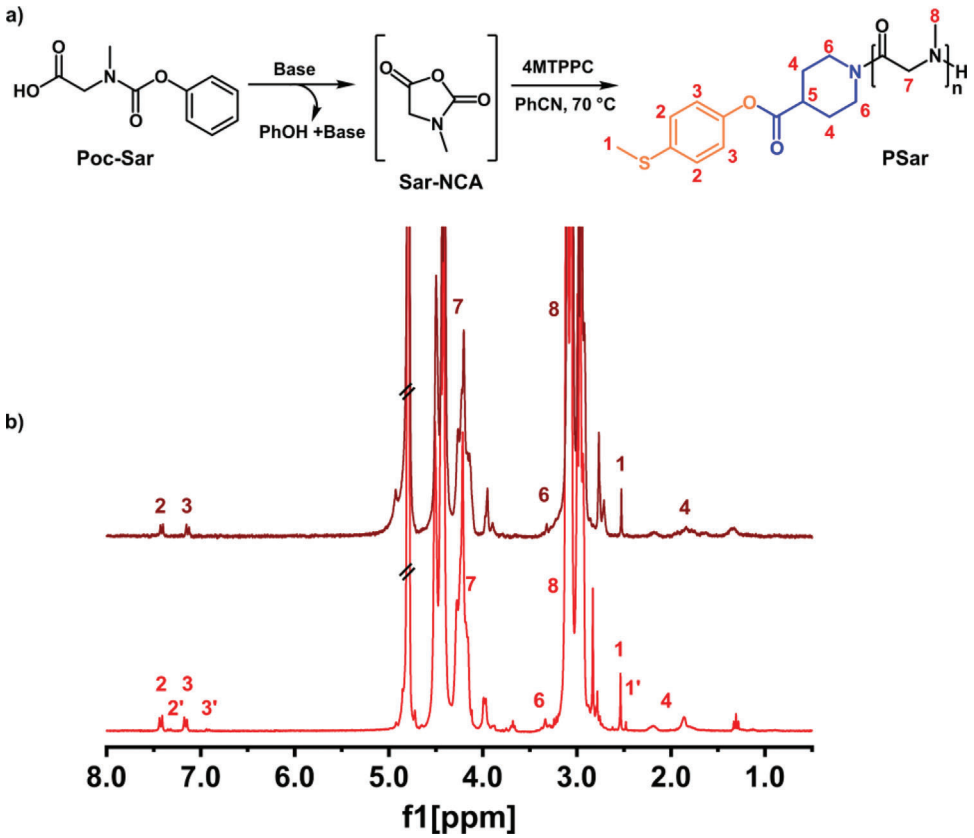

Figure 4. a) Synthesis of polysarcosine through in situ synthesis of N-methylglycine-NCA from an activated urethane precursor in the presence of base and 4-(methylthio)phenyl piperidine-4-carboxylate initiator. b) ^{1}H NMR spectrum (300 MHz, 298 K, D_2O) of the synthesized telechelic polysarcosine obtained by in situ generation of *N*-methylglycine NCA from an activated urethane precursor in the presence of triethylamine and 4-(methylthio)phenol piperidine-4-carboxylate initiator direct after polymerization (top) and stored for several months (bottom).

This can be attributed to a loss of a MeS fragment from the MTP moiety. PSar with a targeted $[M]_0/[I]_0 = 20$ also shows signals attributed to protonated polymer bearing amine terminus (ϵ) as well as their subdistribution bearing potassium ion doping (α) (Figure 5d). The presence of signals that can be attributed to a hydrolyzed α-terminus is also observed with proton (β), potassium (γ), and sodium (δ) ion doping. Signals observed at m/z = 1363 could also be attributed to fragmented 4MTPPC-functionalized polymer bearing sodium (δ) ion doping. PSar with higher $[M]_0/[I]_0$ ($n \geq 30$) show two principal peak distributions. The attribution of the main subdistribution (α) is unfortunately not unambiguous (Figure 5d). The broad signal could be attributed to either a partially hydrolyzed α-terminus or a fragmented 4MTPPC α-termini bearing potassium(α) and sodium (β) ion doping, respectively, or a combination of both. The obtained signals could also be attributed to the desired PSar with a carbamic acid terminus. However, the latter species seems to be improbable, considering that the se rather unstable species have not been reported before for PSar MALDI-ToF mass spectra.

After successful polymerization of Poc-Sar with 4MTPPC, the activation (via oxidation) of the terminal MTP esters was performed. As was reported previously, different reagents can be used for oxidation. Johnson and Jacob treated *N*-carbobenzoxy amino acid MTP esters of lysine, alanine, leucine, etc., with 30% H_2O_2 in glacial acetic acid for 12 h to obtain the corresponding MTO_2P esters.[153,154] However, these conditions were found to be more harsh than needed. Ulbricht et al. found that medium molecular weight PSar ($[M]_0/[I]_0 = 138$) undergoes minor oxidative degradation during treatment with 50×10^{-3} M (< 0.3%) H_2O_2 at 37 °C after 30 min of incubation, therefore oxidative damage to PSar is a potential issue.[66,155] Treatment with 3.0 eq. of *m*-chloroperoxybenzoic acid (*m*-CPBA) in dioxane for 4 h was later found also to convert MTP ester into the activated form.[141] Recently Popovic and colleagues introduced oxone as the oxidizing agent for 4MTP activation.[146] In a slightly different but related approach, Wu et al. reported a very interesting PPM of thiocarbamate derivatives of poly(2-oxazoline)s, which were also oxidized using *m*-CPBA to make them amendable for nucleophilic substitution.[156] Accordingly, we chose to utilize the same strategy to prevent polymer degradation and confirmed that the sulfone is generated under mild conditions with 3.0 eq. *m*-CPBA (**Figure 6**).

^{1}H NMR spectra of the activated polymer confirm the good efficiency of the oxidation. We observe a significant shift of the aromatic signals 2 and 3 (at 7.86 and 7.46 ppm, respectively) before and after oxidation (**Figure 7**a, red) due to an increased electronegativity of the sulfonyl group. Likewise, signal 1, attributed to the methyl group next to sulfide/sulfonyl, is shifted and overlaps with the polymer backbone after oxidation, as was verified by oxidizing the initiator 4-MTPPC as a model compound

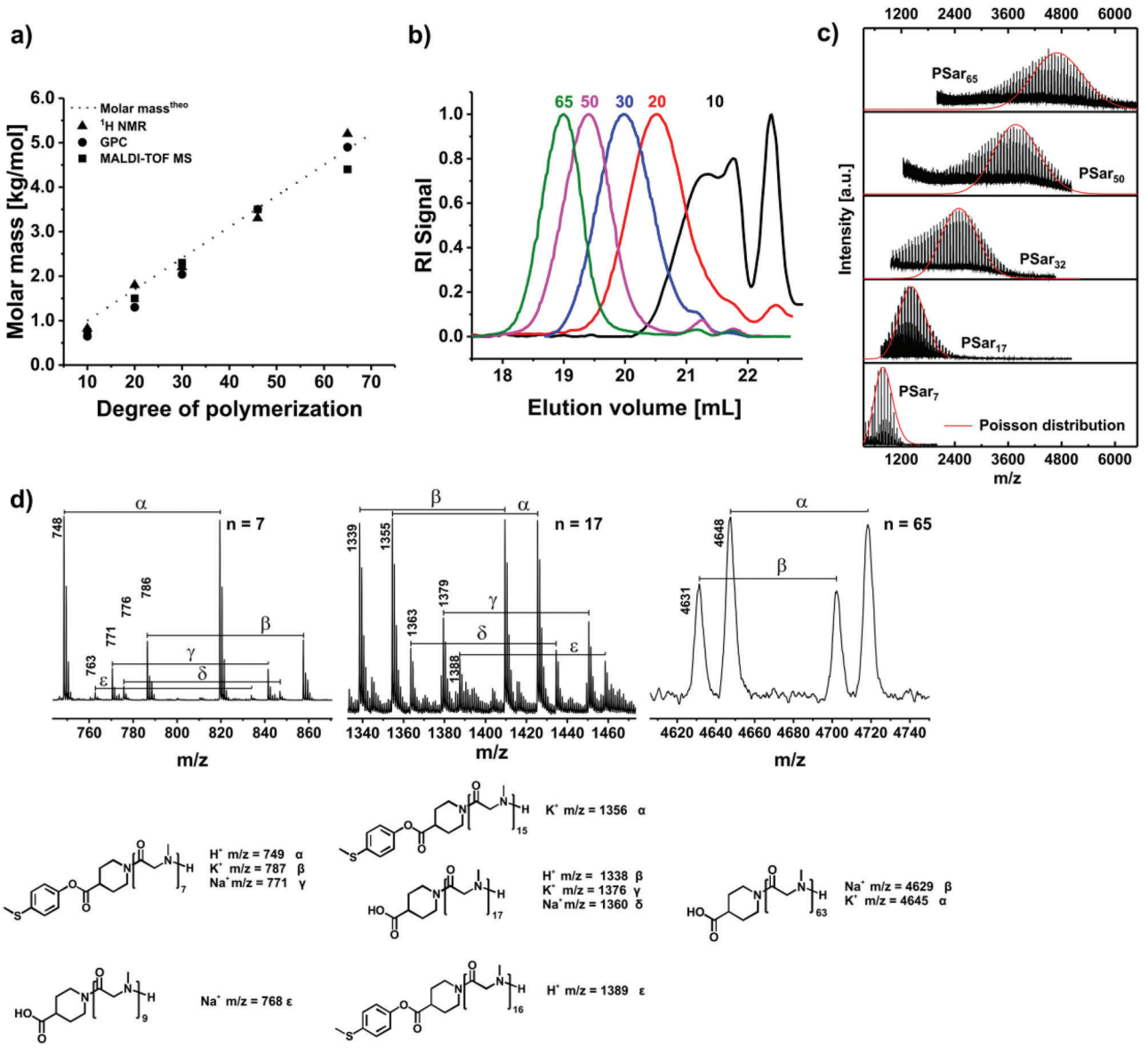

Figure 5. Overview on the characterization of 4MTPPC functionalized polymers. a) Correlation of experimentally determined and theoretical values of molar masses of polymers with different $[M]_0/[I]_0$. b) GPC traces of the 4MTPPC-functionalised polysarcosines with different $[M]_0/[I]_0$. c) MALDI-ToF spectra of the resulting polysarcosines and calculated Poisson distribution. The disperse distributions are overlaid with the respective Poisson distributions (red curve). d) Zoom into maximum of the molar mass distribution of the $[M]_0/[I]_0 = 10$, 20, and 70 and assignment of chemical structures to respective m/z ratios.

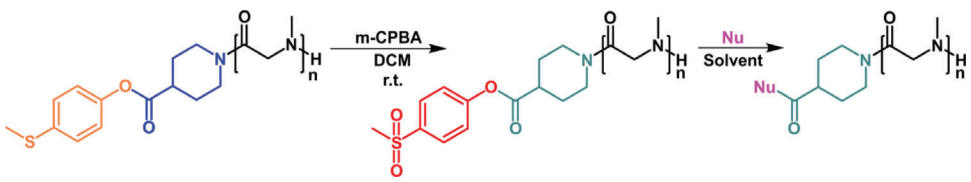

Figure 6. Schematic illustration of the activation of 4MTPPC-functionalized polysarcosine via oxidation with 3.0 eq. of m-chloroperoxybenzoic acid and further postpolymerization modification.

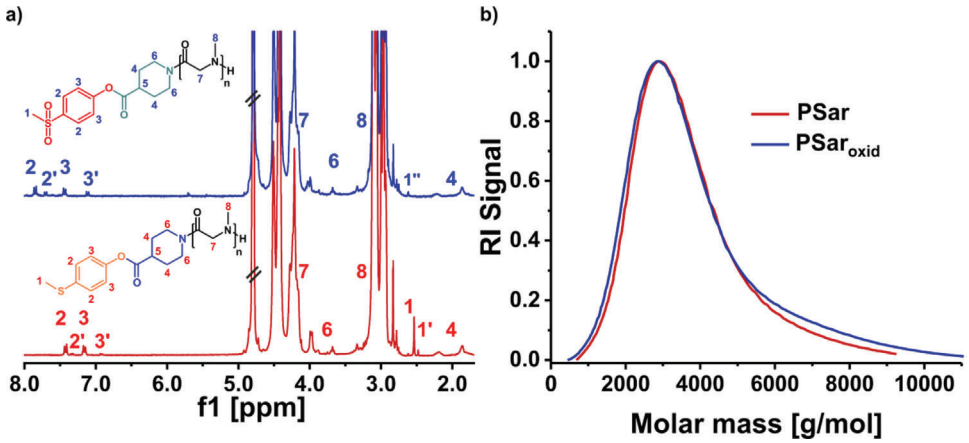

Figure 7. Characterization of the 4MTPPC-functionalized polysarcosine by a) ^{1}H NMR spectra (300 MHz, 297 K, D_2O) and b) GPC traces before (blue) and after oxidation (red).

(see Figure S6, Supporting Information,). As the MTP ester is prone to hydrolysis, particularly after oxidation, we also find signals that can be attributed to a hydrolyzed terminal group. In particular, signals 2' and 3' (at 7.71 and 7.13 ppm, respectively) (Figure 7a, red) are attributed to 4-(methylsulfonyl)phenol, cleaved off the polymer via hydrolysis. The signal 1" (at 2.64 ppm) is attributed to the methyl group next to the sulfoxide (partially oxidized MTP), even though we did not observe the other signals expected for the partly oxidized phenyl ring.

GPC traces of the oxidized polymer remained monomodal, narrow and M_n remained essentially unchanged (Figure 7b), which indicates that polymer degradation or cross-linking is very limited or does not occur.[66,155] It should be noted, when we increased the oxidation time up to 24 h, GPC analysis suggests polymer degradation as evidenced by a decrease of the molar mass, as well as the presence of the high molecular weight shoulder pointing to the coupling of polymer chains (Figure S7, Supporting Information).

After successful activation to yield oxidized PSar (PSar$_{oxid}$), we performed nucleophilic substitution with different low and higher molecular weight *N*-and *S*-nucleophiles. In the first experiments, PSar$_{oxid}$ was incubated with 3.0 eq. of *N*-nucleophile (neopentylamine, benzylamine, and dansylcadaverine) overnight, showing a satisfying degree of functionalization (89%, 78.1%, and 65%, respectively) (**Figure 8**a). ^{1}H NMR spectra of PSar$_{oxid}$ treated with benzylamine in MeCN shows a new signal at 7.50 ppm attributed to the phenyl ring of *α*-benzylamine-PSar (Figure 8a). Neopentylamine modified PSar (*α*-neopentylamine-PSar) shows the significant shift of the signal 10' at 0.89 ppm (attributed to free neopentylamine) to 1.04 ppm (signal 10), confirming the successful functionalization (Figure 8b). PPM with dansylcadaverine was performed in DMSO under the same conditions following purification by precipitation from cold diethyl ether (3 times) and subsequent gel filtration (LH-20 with MeOH as eluent). The ^{1}H NMR spectra of *α*-dansylcadaverin-PSar shows new signals at 7.10–8.5 ppm (signals 12–17) attributed to aromatic moieties of dansylcadaverine (Figure 8c), while signals 9–11 were not distinguishable in the ^{1}H NMR spectra. However, we still observed signals at 7.5–7.8 ppm (Figure 8a,b, red frame) possibly attributed to unoxidized PSar (however, the oxidative analysis shows that utilized conditions are enough for complete PSar oxidation) or to the presence of the residual alcohol.

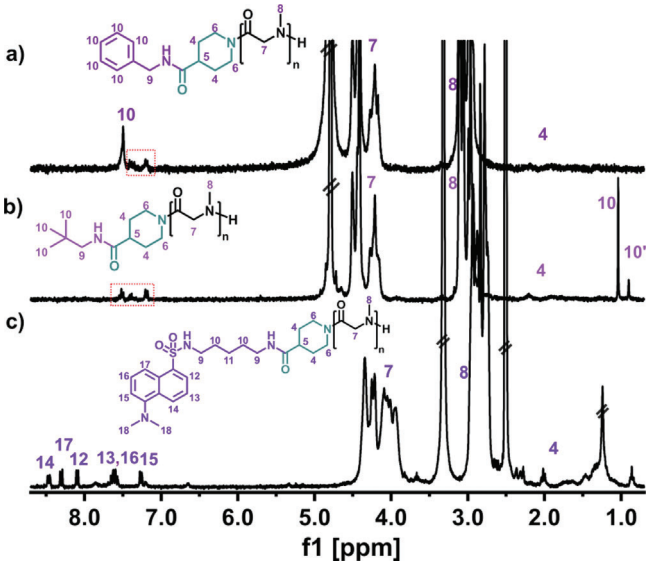

Figure 8. ^{1}H NMR (300 MHz, 297 K, D_2O, and DMSO) of modification of the activated polysarcosines with benzylamine a), neopentylamine b) and dansylcadaverine c).

MALDI-ToF MS data corroborate the functionalization of PSar with the low molecular weight nucleophiles (**Figure 9**). In the mass spectra of the *α*-benzylamine-PSar, signals attributed to the desired product featuring an amine *ω*-terminus and sodium (*γ*) and potassium (*α*) ion doping, respectively (Figure 9a), are observed. We also observed signals that can be attributed to oxidized PSar with proton (*δ*) ion doping. Signals at m/z = 3711 could be attributed to the PSar starting material that underwent fragmentation and sodium (*β*) ion doping. Signals suggesting the presence of PSar with a hydrolyzed MTP ester and sodium ion doping (*ϵ*) were also detected.

An analysis of *α*-neopentylamine-PSar showed the presence of signals that can be attributed to the product bearing proton (*ω*), sodium (*δ*), and potassium (*α*) ion doping with amine

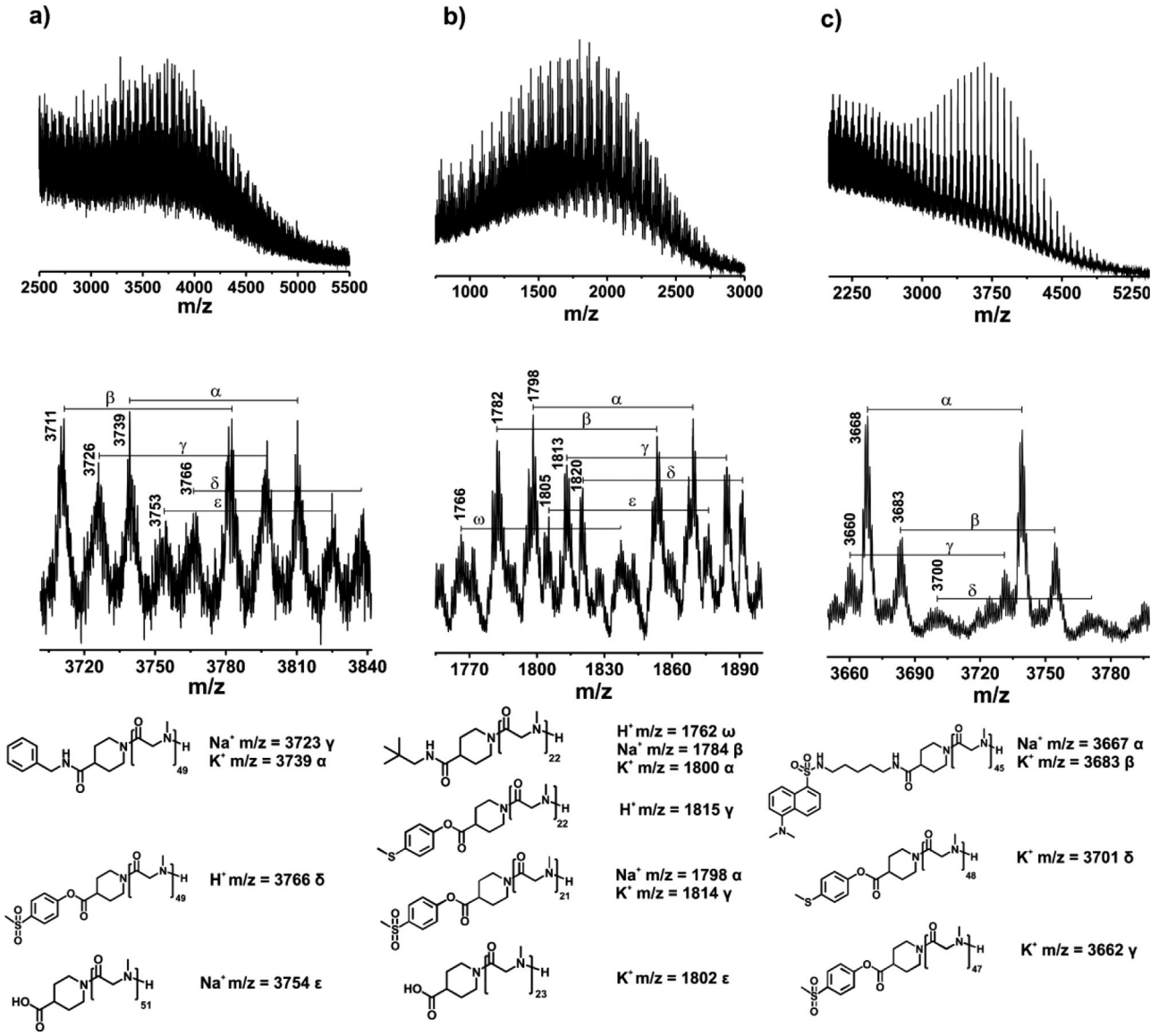

Figure 9. MALDI-ToF mass spectra and structural assignment of m/z ratio for benzylamine a), neopentylamine b), and dansylcadaverine c) functionalized polysarcosines.

ω-termini (Figure 9b). However, we also observed signals that could be attributed to unoxidized PSar (γ) or $PSar_{oxid}$ bearing sodium (α) or potassium (γ) ion doping with an amine ω-terminus. Signals with lower intensity can be assigned to PSar with hydrolyzed 4MTPPC-α-termini bearing potassium (ϵ) ion doping. The weaker δ distribution may be attributed to fragmented PSar chains.

Successful functionalization with dansylcadaverine is evidenced by the two most intense signals in the MS at m/z = 3668 and 3683, which can be attributed to the desired product ionized with Na^+ (α) and K^+ (β), respectively, featuring an amine ω-terminus. The weaker γ and δ distributions can be attributed to residual PSar and $PSar_{oxid}$ bearing potassium ion doping, respectively (Figure 9c).

Additionally, the UV–vis spectra of $PSar_{Dansyl}$ show a strong absorbance at 335 nm attributed to the presence of dansylcadaverine, which was not observed in the precursor polymers (Figure S8, Supporting Information). Quantification of the polymer conjugated dye from UV-vis was in excellent correlation with expected values (calculated efficiency of functionalisation is 95%), corroborating the potential to apply the proposed method for PPM.

As a next step, we tested the more challenging conjugation with bio(macro)molecules, such as peptides and proteins. The activated polymer was incubated with glutathione as a model peptide, red fluorescent protein (RFP) and bovine serum albumin (BSA) as model proteins. The conjugation was performed in phosphate buffer solution (PBS) at pH = 8 for 4–5 h.

Glutathione (GSH) was chosen due to its antioxidant properties and the presence of two available nucleophilic groups that can, in theory, react with the activated ester group of $PSar_{oxid}$. As expected, GPC traces of the resulting product ($PSar_{GHS}$) after

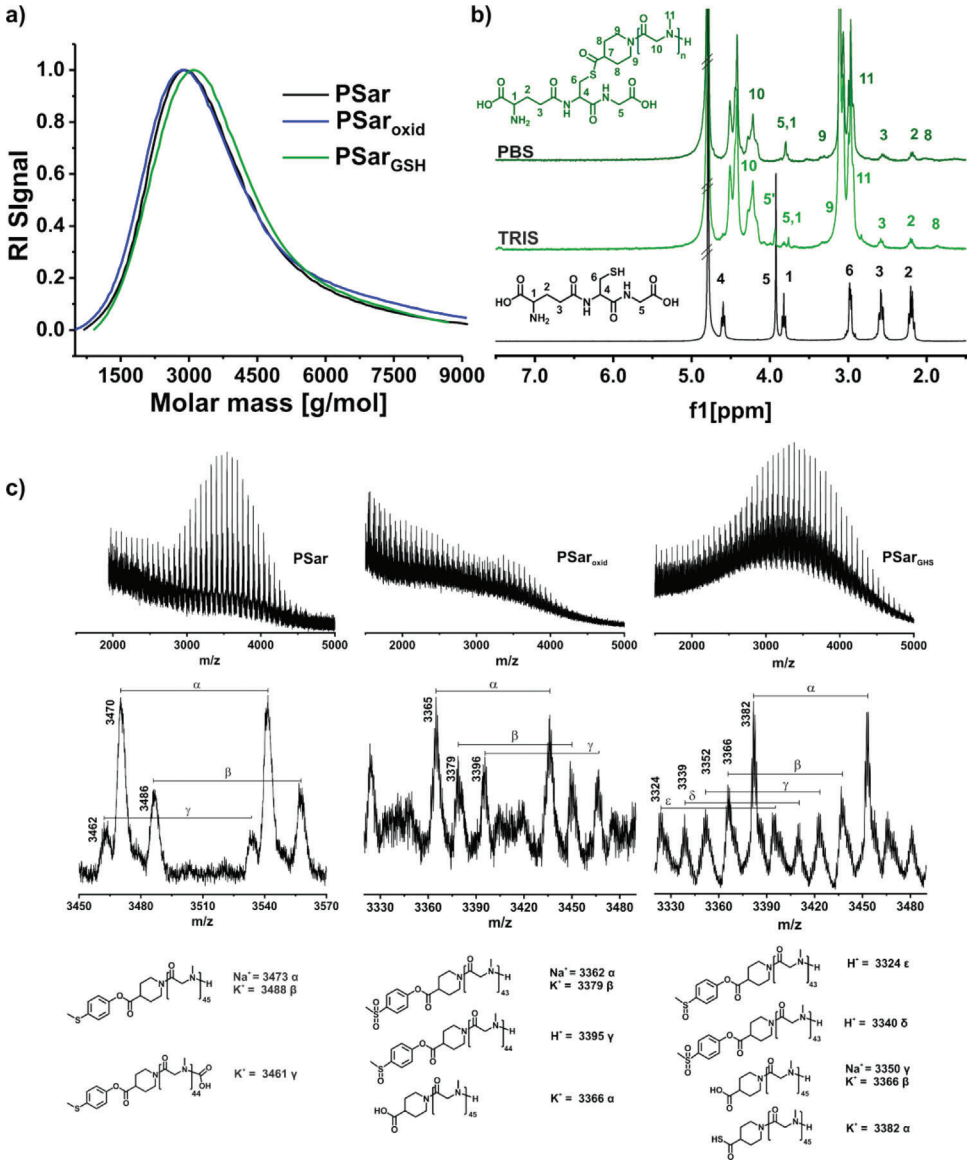

Figure 10. Functionalisation of activated polysarcosine with glutathione (GHS). a) HFIP GPC traces of the protected polysarcosine (black), activated/oxidized polymer (blue) and glutathione conjugated polymer. b) ^{1}H NMR spectra (300 MHz, 297 K, D_2O) of free glutathione (black) and glutathione conjugated polymer (green) in PBS and TRIS buffer solution, respectively. c) MALDI-ToF mass spectra and structural assignment of m/z ratio for glutathione functionalized polysarcosines.

incubation demonstrate a slight but noticeable difference between the respective elution volumes (**Figure 10**a). The presence of a new signal at 3.80 ppm in the ^{1}H NMR spectra also substantiates a successful reaction (Figure 10b). An overlay of the ^{1}H NMR spectra of PSar$_{GHS}$ and GHS showed that the shifting of the signals 1 and 5 depends on the used buffer solution. After incubation in the TRIS-HCl buffer, signal 1 shifted toward lower ppm values and a new signal at 3.80 ppm is observed, while signal 5 appears to split into two signals.

In contrast, incubation in PBS leads to a shift of the signals 1 and 5 to lower ppm values and both signals appear to overlap. Such low ppm shifting can result from the hydrogen bonds in the water solution.[157] Unfortunately, signals 4 and 6 could not be unambiguously assigned in NMR spectra, either due to low intensity or overlap with the broad and intense signal of the polymer side chain. Important to note, the same peak shifting is observed after the reaction between oxidized 4MTPPC (4MPTO$_2$PC) and GHS (Figure S9, Supporting Information). Signal 5 shifts completely after incubation in PBS but not TRIS-HCl. In addition, after conjugation in TRIS-HCl, signal 6 remains largely unchanged, it essentially disappears after incubation in PBS.

The presence of side reactions such as cyclization[158] or rapid hydrolysis of resulting thioester bonds cannot be excluded. Mitamura et al. reported on the rapid hydrolysis of the thioester bond in GHS conjugated products and reports the presence of a thiocarboxylic acid and an elimination product of the thioester in mass spectra.[159] Here, MALDI-ToF mass spectrometry was performed to confirm the successful GHS conjugation.

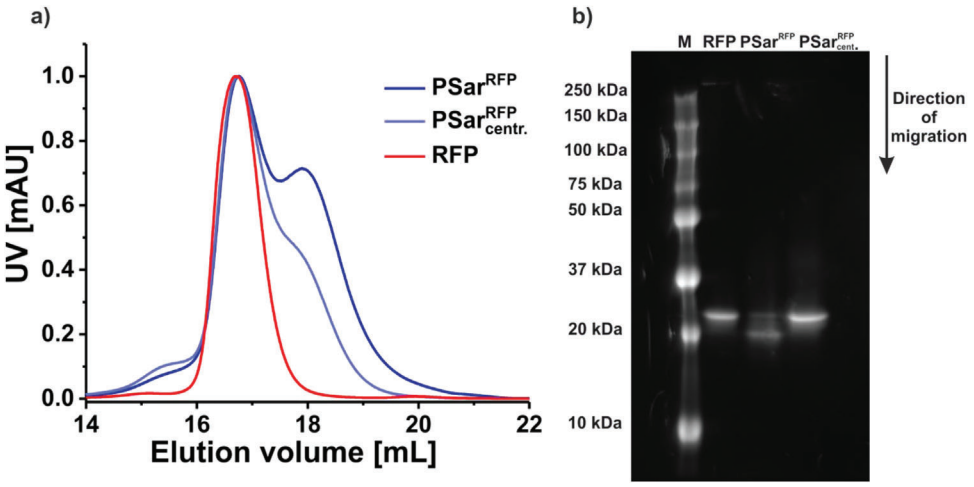

Figure 11. Conjugation of activated polymers with red fluorescent protein (RFP) a) FPLC traces of the PSar conjugated with RFP (λ = 280 nm). b) Visualization of $PSar_{RFP}$ conjugation using polyacrylamide gel electrophoresis (PAGE). Protein molecular weight standards (M); native red fluorescent protein (RFP); reaction mixture of $PSar_{oxid}$ and RFP after conjugation ($PSar_{RFP}$); reaction mixture of $PSar_{oxid}$ and RFP after conjugation and purification via centrifugation with centrifugal filter (pore size is 10 kg mol^{-1}) ($PSar_{centr.}^{RFP}$).

Interestingly, compared to $PSar_{oxid}$, the MALDI-ToF MS of $PSar_{GHS}$ is much better resolved again and gives a clear and narrow m/z distribution. While we could not attribute signals of the fully desired GHS conjugate PSar, the most intense distribution can be attributed to a thiocarboxylic acid fragment with a K^+ (α) ion doping (Figure 10c). We suppose that resulting $PSar_{GHS}$ is not ionized efficiently itself but rather degrades during MALDI-ToF analysis. However, also the presence of the signals attributed to partly oxidized (ϵ) and oxidized (δ) PSar with amine ω-termini as well as partly hydrolyzed PSar bearing sodium (γ) and potassium (β) ion doping is observed (Figure 10c). The presence of the $PSar_{oxid}$ clearly shows that the conversion is not the complete under the chosen conditions.

Results obtained after conjugation with a red fluorescent protein (RFP) were found to be less successful. RFP was incubated with $PSar_{oxid}$ (with 1:5 ratio, respectively) in PBS (pH = 8.0) for 4 h. The resulting product ($PSar_{RFP}$) was purified with a centrifugal filter (CF) and analyzed with FPLC (**Figure 11**a) and PAGE techniques (Figure 11b).

Judging from FPLC traces before and after conjugation (Figure 11a), only a minor fraction of RFP was conjugated with PSar, as evidenced by a minor shoulder at lower elution volumes. The $PSar_{RFP}$ reaction mixture is represented with two clear signals attributed to excessed $PSar_{oxid}$ and conjugated RFP (Figure 11a, dark blue). This unexpected observation could be related either to inferior conjugation degree or decreased $PSar_{RFP}$ hydrodynamic radius after functionalization. A noticeable decrease of the second peak and increased molecular weight shoulder after centrifugation (most molecules lower than 10.0 kg mol^{-1} were removed) are observed (Figure 11a, blue). Side reactions could also explain the presence of the high molecular shoulder in $PSar_{RFP}$ traces during conjugation. PAGE analysis shows that electrophoretic patterns of RFP alone exhibit a characteristic band at ≈25 kg mol^{-1}, while the conjugated $PSar_{RFP}$ before centrifugation shows three prominent bands that could be attributed to free RFP and the desired $PSar_{RFP}$ that appeared at lower $M_{w,}$ which suggesting that presence of PBS increases the migration rate of $PSar_{RFP}$ (Figure 11b). PAGE of the purified $PSar_{RFP}$ shows only one band at the same region that native RFP but no minor smear at higher M_w (Figure 11b) (Figure S10, Supporting Information,). We expect that reaction conditions critically influence the degree of conjugation and that further improvements are needed. BSA was selected as another model protein for conjugation due to its ready availability, robust nature, and the presence of an accessible free thiol at Cys-34 and 60 free amine groups available for conjugation.[160–162] The conjugation method uses a large excess of $PSar_{oxid}$ (M_w = 3.5 kg mol^{-1}). The experiment was carried out for 5 and 72 h in PBS at pH = 8.0. Subsequently, the reaction mixture was dialyzed against water for 4 to remove unreacted polymer before lyophilization. GPC analysis shows a minor shift after 5 h and a significant tailing at higher molar mass after 72 h (**Figure 12**a). The negligible molar mass difference between $PSar_{BSA}$ and native BSA suggests that the conjugation via the amine group is avoided under these pH conditions, and only cysteine group is available for interaction. In fact, it has been reported that at neutral or mild alkaline pH the free cysteine group is available for conjugation, while the conjugation via the amino groups of lysine is avoided,[163–165] supporting our suggestion. $PSar_{BSA}$ incubated for 72 h shows higher molecular weight tailing compared with native BSA and, also, presence of low molecular weight tailing for signal attributed to $PSar_{oxid}$ (Figure 12a). The presence of tailing points that increased incubation time leads to increased side reactions with $PSar_{oxid}$, such as chain coupling or degradation and increases the degree of conjugation (Figure 12a). The SDS-PAGE analysis of $PSar_{BSA}$ performed after coupling in PBS at pH = 8.5 ($PSar_{BSA1}$) and 11 ($PSar_{BSA2}$) demonstrate successful coupling. A small but distinct increase in molar mass was found between BSA and its corresponding conjugates ($PSar_{BSA1}$ and $PSar_{BSA2}$), respectively. The average molar mass was estimated to be ≈75–80 kg mol^{-1} (Figure S11, supporting information). Our results suggest that the degree of conjugation depends on the pH of the reaction media (Figure 12), which is well known for the reaction of activated carboxylic acids. The difference in band intensity points that significant excess of

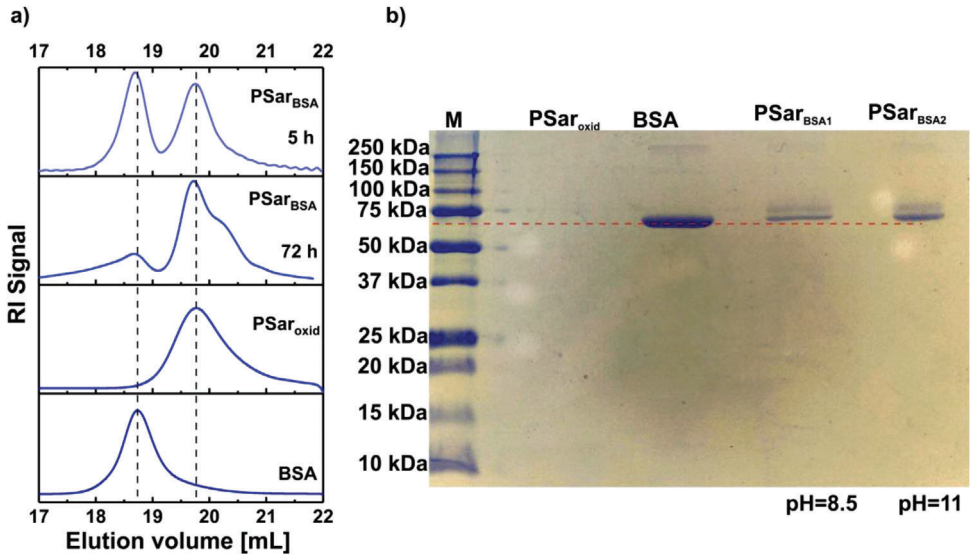

Figure 12. a) Water GPC traces of the bovine serum albumin conjugated polysarcosine. b) Visualization of bovine serum albumin conjugate using sodium dodecyl sulphate–polyacrylamide gel electrophoresis (SDS-PAGE). Protein molecular weight standards (M); native oxidized polysarcosine (PSar$_{oxid}$); native bovine serum albumin (BSA) bovine serum albumin conjugate performed at pH = 8.5 (PSar$_{BSA1}$) and bovine serum albumin conjugate performed at pH = 11 (PSar$_{BSA2}$).

unreacted PSar is present even after 24 h of dialysis (membrane pore size is 10 kDA).

4. Conclusions

This study describes the first synthesis of a functional and activatable initiator for the living ring-opening polymerization of *N*-carboxyanhydrides. Well-defined functionalized PSar bearing this initiator can be activated via oxidation (using m-CPBA) and utilized for postpolymerization modification with different –SH and –NH_2 nucleophiles of low and high molecular weight nucleophiles, including bovine serum albumin as a model protein. Successful functionalization was demonstrated by NMR spectroscopy, GPC, FPLC, SDS-PAGE, and MALDI-ToF spectrometry. The efficiency of aminolysis over hydrolysis depends on the solvent, temperature, reactants etc. Here, all PPM were performed at room temperatures at slightly basic or neutral pH. Future work should concentrate on the improvement of the reaction conditions to overcome the current limitations.

Even though there are limitations due to occurring hydrolysis of the functionalized group during storage and imperfect conjugation, we believe that the introduced method is a valuable tool for the postpolymerization bioconjugation of polypeptides and polypeptoids and could also be extended to other classes of polymers.

Supporting Information

Supporting Information is available from the Wiley Online Library or from the author.

Acknowledgements

S.B. would like to thank the Bavarian Academic Center for Central, Eastern and Southeastern Europe (BAYHOST) for scholarship support. The authors also thank the Deutsche Forschungsgemeinschaft for financial support (Project No. 329144954, awarded to R.L.).

Open Access funding enabled and organized by Projekt DEAL.

Conflict of Interest

The authors declare no conflict of interest.

Data Availability Statement

The data that support the findings of this study are available in the supplementary material of this article.

Keywords

bioconjugation, functional initiators, polypeptoids, postpolymerization modification, ring-opening polymerization

Received: September 4, 2021
Revised: November 8, 2021
Published online: January 7, 2022

[1] A. Kakkar, G. Traverso, O. C. Farokhzad, R. Weissleder, R. Langer, *Nat. Rev. Chem.* **2017**, *1*, 1.
[2] O. Sedlacek, R. Hoogenboom, *Adv. Ther.* **2020**, *3*, 1900168.
[3] W. Chen, S. Zhou, L. Ge, W. Wu, X. Jiang, *Biomacromolecules* **2018**, *19*, 1732.
[4] Z. Yang, D. Gao, Z. Cao, C. Zhang, D. Cheng, J. Liu, X. Shuai, *Biomater. Sci.* **2015**, *3*, 1035.
[5] N. Nishiyama, K. Kataoka, *Pharmacol. Ther.* **2006**, *112*, 630.
[6] S. Datta, A. Jutková, P. Srámková, L. Lenkavská, V. Huntošová, D. Chorvát, P. Miškovský, D. Jancura, J. Kronek, *Biomacromolecules* **2018**, *19*, 2459.

[7] O. Koshkina, T. Lang, R. Thiermann, D. Docter, R. H. Stauber, C. Secker, H. Schlaad, S. Weidner, B. Mohr, M. Maskos, *Langmuir* **2015**, *31*, 8873.
[8] A. Zinger, L. Koren, O. Adir, M. Poley, M. Alyan, Z. Yaari, N. Noor, N. Krinsky, A. Simon, H. Gibori, *ACS Nano* **2019**, *13*, 11008.
[9] S. Grabbe, K. Landfester, D. Schuppan, M. Barz, R. Zentel, *Nanomedicine* **2016**, *11*, 2621.
[10] S. S. Nogueira, A. Schlegel, K. Maxeiner, B. Weber, M. Barz, M. A. Schroer, C. E. Blanchet, D. I. Svergun, S. Ramishetti, D. Peer, *ACS Appl. Nano Mater.* **2020**, *3*, 10634.
[11] H. Unterweger, R. Tietze, C. Janko, J. Zaloga, S. Lyer, S. Dürr, N. Taccardi, O.-M. Goudouri, A. Hoppe, D. Eberbeck, D. W. Schoubert, A. R. Boccaccini, C. Alexiou, *Int. J. Nanomed.* **2014**, *9*, 3659.
[12] V. Marzaioli, J. A. Aguilar-Pimentel, I. Weichenmeier, G. Luxenhofer, M. Wiemann, R. Landsiedel, W. Wohlleben, S. Eiden, M. Mempel, H. Behrendt, *Int. J. Nanomed.* **2014**, *9*, 2815.
[13] A. Schulz, A. Stocco, A. Bethry, J. P. Lavigne, J. Coudane, B. Nottelet, *Adv. Funct. Mater.* **2018**, *28*, 1800976.
[14] F. Siedenbiedel, J. C. Tiller, *Polymers* **2012**, *4*, 46.
[15] S. Li, S. Dong, W. Xu, S. Tu, L. Yan, C. Zhao, J. Ding, X. Chen, *Adv. Sci.* **2018**, *5*, 1700527.
[16] A. Alzagameem, S. E. Klein, M. Bergs, X. T. Do, I. Korte, S. Dohlen, C. Hüwe, J. Kreyenschmidt, B. Kamm, M. Larkins, M. Schulze, *Polymers* **2019**, *11*, 670.
[17] A. Jain, L. S. Duvvuri, S. Farah, N. Beyth, A. J. Domb, W. Khan, *Adv. Healthcare Mater.* **2014**, *3*, 1969.
[18] J. Yoo, A. Birke, J. Kim, Y. Jang, S. Y. Song, S. Ryu, B.-S. Kim, B.-G. Kim, M. Barz, K. Char, *Biomacromolecules* **2018**, *19*, 1602.
[19] D. Wang, G. Tong, R. Dong, Y. Zhou, J. Shen, X. Zhu, *Chem. Commun.* **2014**, *50*, 11994.
[20] Y. Zhou, W. Huang, J. Liu, X. Zhu, D. Yan, *Adv. Mater.* **2010**, *22*, 4567.
[21] Z.-X. Zhang, X. Liu, F. J. Xu, X. J. Loh, E.-T. Kang, K.-G. Neoh, J. Li, *Macromolecules* **2008**, *41*, 5967.
[22] I. W. Hamley, *Biomacromolecules* **2014**, *15*, 1543.
[23] A. Birke, J. Ling, M. Barz, *Prog. Polym. Sci.* **2018**, *81*, 163.
[24] S. H. Petrosko, R. Johnson, H. White, C. A. Mirkin, *J. Am. Chem. Soc.* **2016**, *138*, 7443.
[25] K. T. Kim, S. A. Meeuwissen, R. J. Nolte, J. C. van Hest, *Nanoscale* **2010**, *2*, 844.
[26] J.-H. Kim, K. Park, H. Y. Nam, S. Lee, K. Kim, I. C. Kwon, *Prog. Polym. Sci.* **2007**, *32*, 1031.
[27] S. Krishnan, C. J. Weinman, C. K. Ober, *J. Mater. Chem.* **2008**, *18*, 3405.
[28] W. K. Cho, S. M. Kang, J. K. Lee, *J. Nanosci. Nanotechnol.* **2014**, *14*, 1231.
[29] Z. Zhang, V. E. Wagner, *Antimicrobial Coatings and Modifications on Medical Devices*, 1st ed., Springer, Cham **2017**.
[30] S. Cichosz, A. Masek, M. Zaborski, *Polym. Test.* **2018**, *67*, 342.
[31] E. Schoolaert, R. Hoogenboom, K. De Clerck, *Adv. Funct. Mater.* **2017**, *27*, 1702646.
[32] B. Guo, P. X. Ma, *Biomacromolecules* **2018**, *19*, 1764.
[33] J. Malda, J. Visser, F. P. Melchels, T. Jüngst, W. E. Hennink, W. J. Dhert, J. Groll, D. W. Hutmacher, *Adv. Mater.* **2013**, *25*, 5011.
[34] R. Censi, W. Schuurman, J. Malda, G. Di Dato, P. E. Burgisser, W. J. Dhert, C. F. Van Nostrum, P. Di Martino, T. Vermonden, W. E. Hennink, *Adv. Funct. Mater.* **2011**, *21*, 1833.
[35] V. A. Ganesh, A. Baji, S. Ramakrishna, *RSC Adv.* **2014**, *4*, 53352.
[36] M. A. Gauthier, M. I. Gibson, H. A. Klok, *Angew. Chem., Int. Ed.* **2009**, *48*, 48.
[37] H. Palza, P. A. Zapata, C. Angulo-Pineda, *Materials* **2019**, *12*, 277.
[38] J. M. Harris, in *Poly(Ethylene Glycol) Chemistry. Topics in Applied Chemistry* (Ed: J. M. Harris), Springer US, Boston, MA **1992**, pp. 1–14.
[39] J. W. Johnson, *Int. J. Toxicol.* **2001**, *20*, 13.
[40] K. Knop, R. Hoogenboom, D. Fischer, U. S. Schubert, *Angew. Chem., Int. Ed.* **2010**, *49*, 6288.
[41] Y. Qin, Y. Zhu, X. Luo, S. Liang, J. Wang, L. Zhang, *Int. J. Energy Res.* **2019**, *43*, 1000.
[42] Y. Inada, K. Takahashi, T. Yoshimoto, A. Ajima, A. Matsushima, Y. Saito, *Trends Biotechnol.* **1986**, *4*, 190.
[43] U. Raviv, J. Frey, R. Sak, P. Laurat, R. Tadmor, J. Klein, *Langmuir* **2002**, *18*, 7482.
[44] R. P. Garay, R. El-Gewely, J. K. Armstrong, G. Garratty, P. Richette, *Expert Opin. Drug Delivery* **2012**, *9*, 1319.
[45] A. W. Richter, E. Åkerblom, *Int. Arch. Allergy Immunol.* **1983**, *70*, 124.
[46] J. K. Armstrong, G. Hempel, S. Koling, L. S. Chan, T. Fisher, H. J. Meiselman, G. Garratty, *Cancer* **2007**, *110*, 103.
[47] M. A. Becker, H. S. Baraf, R. A. Yood, A. Dillon, J. Vázquez-Mellado, F. D. Ottery, D. Khanna, J. S. Sundy, *Ann. Rheum. Dis.* **2013**, *72*, 1469.
[48] J. Scheirs, S. W. Bigger, O. Delatycki, *Polymer* **1991**, *32*, 2014.
[49] S. Morlat, J.-L. Gardette, *Polymer* **2001**, *42*, 6071.
[50] C. A. Stone Jr, Y. Liu, M. V. Relling, M. S. Krantz, A. L. Pratt, A. Abreo, J. A. Hemler, E. J. Phillips, *J. Allergy Clin. Immunol.* **2019**, *7*, 1533.
[51] E. Wenande, L. Garvey, *Clin. Exp. Allergy* **2016**, *46*, 907.
[52] C. Conover, L. Lejeune, R. Linberg, K. Shum, R. G. Shorr, *Artif. Cells Nanomed. Biotechnol.* **1996**, *24*, 599.
[53] D. G. Rudmann, J. T. Alston, J. C. Hanson, S. Heidel, *Toxicol. Pathol.* **2013**, *41*, 970.
[54] https://www.fda.gov/media/104091/download (accessed January 2021).
[55] F. Zhang, M.-R. Liu, H.-T. Wan, *Biol. Pharm. Bull.* **2014**, *37*, 335.
[56] N. J. Ganson, T. J. Povsic, B. A. Sullenger, J. H. Alexander, S. L. Zelenkofske, J. M. Sailstad, C. P. Rusconi, M. S. Hershfield, *J. Allergy Clin. Immunol.* **2016**, *137*, 1610.
[57] N. E. Elsadek, E. Hondo, T. Shimizu, H. Takata, A. S. Abu Lila, S. E. Emam, H. Ando, Y. Ishima, T. Ishida, *Mol. Pharmaceutics* **2020**, *17*, 2964.
[58] I. Hamad, A. Hunter, J. Szebeni, S. M. Moghimi, *Mol. Immunol.* **2008**, *46*, 225.
[59] X.-D. Zhang, X. S. Di Wu, P.-X. Liu, N. Yang, B. Zhao, H. Zhang, Y.-M. Sun, L.-A. Zhang, F.-Y. Fan, *Int. J. Nanomed.* **2011**, *6*, 2071.
[60] L. Zhao, J. Kong, N. Krasteva, D. Wang, *Toxicol. Res.* **2018**, *7*, 1061.
[61] L. H. Garvey, S. Nasser, *Br. J. Anaesth.* **2021**, *126*, e106.
[62] M. C. Castells, E. J. Phillips, *N. Engl. J. Med.* **2021**, *384*, 643.
[63] P. J. Turner, I. J. Ansotegui, D. E. Campbell, V. Cardona, M. Ebisawa, E.-G. Yehia, S. Fineman, M. Geller, A. Gonzalez-Estrada, P. A. Greenberger, *World Allergy Organ. J.* **2021**, *14*, 100517.
[64] S. Bleher, J. Buck, C. Muhl, S. Sieber, S. Barnert, D. Witzigmann, J. Huwyler, M. Barz, R. Süss, *Small* **2019**, *15*, 1904716.
[65] T. Lorson, M. M. Lübtow, E. Wegener, M. S. Haider, S. Borova, D. Nahm, R. Jordan, M. Sokolski-Papkov, A. V. Kabanov, R. Luxenhofer, *Biomaterials* **2018**, *178*, 204.
[66] J. Ulbricht, R. Jordan, R. Luxenhofer, *Biomaterials* **2014**, *35*, 4848.
[67] M. Barz, R. Luxenhofer, R. Zentel, M. J. Vicent, *Polym. Chem.* **2011**, *2*, 1900.
[68] H. Zhu, Y. Chen, F.-J. Yan, J. Chen, X.-F. Tao, J. Ling, B. Yang, Q.-J. He, Z.-W. Mao, *Acta Biomater.* **2017**, *50*, 534.
[69] X. Tao, C. Deng, J. Ling, *Macromol. Rapid Commun.* **2014**, *35*, 875.
[70] Y. Deng, T. Zou, X. Tao, V. Semetey, S. Trepout, S. Marco, J. Ling, M.-H. Li, *Biomacromolecules* **2015**, *16*, 3265.
[71] C. Hörtz, A. Birke, L. Kaps, S. Decker, E. Wächtersbach, K. Fischer, D. Schuppan, M. Barz, M. Schmidt, *Macromolecules* **2015**, *48*, 2074.
[72] Y. Hu, Y. Hou, H. Wang, H. Lu, *Bioconjugate Chem.* **2018**, *29*, 2232.
[73] C. W. Wu, T. J. Sanborn, K. Huang, R. N. Zuckermann, A. E. Barron, *J. Am. Chem. Soc.* **2001**, *123*, 6778.
[74] K. Kirshenbaum, A. E. Barron, R. A. Goldsmith, P. Armand, E. K. Bradley, K. T. Truong, K. A. Dill, F. E. Cohen, R. N. Zuckermann, *Proc. Natl. Acad. Sci. USA* **1998**, *95*, 4303.

[75] K. Klinker, M. Barz, *Macromol. Rapid Commun.* **2015**, *36*, 1943.
[76] D. Zhang, S. H. Lahasky, L. Guo, C.-U. Lee, M. Lavan, *Macromolecules* **2012**, *45*, 5833.
[77] S. H. Lahasky, X. Hu, D. Zhang, *ACS Macro Lett.* **2012**, *1*, 580.
[78] A. Li, D. Zhang, *Biomacromolecules* **2016**, *17*, 852.
[79] P. Heller, A. Birke, D. Huesmann, B. Weber, K. Fischer, A. Reske-Kunz, M. Bros, M. Barz, *Macromol. Biosci.* **2014**, *14*, 1380.
[80] B. Weber, C. Seidl, D. Schwiertz, M. Scherer, S. Bleher, R. Süss, M. Barz, *Polymers* **2016**, *8*, 427.
[81] S. Varlas, P. G. Georgiou, P. Bilalis, J. R. Jones, N. Hadjichristidis, R. K. O'Reilly, *Biomacromolecules* **2018**, *19*, 4453.
[82] M. Schneider, Z. Tang, M. Richter, C. Marschelke, P. Förster, E. Wegener, I. Amin, H. Zimmermann, D. Scharnweber, H. G. Braun, *Macromol. Biosci.* **2016**, *16*, 75.
[83] K. H. A. Lau, C. Ren, T. S. Sileika, S. H. Park, I. Szleifer, P. B. Messersmith, *Langmuir* **2012**, *28*, 16099.
[84] S. Cui, X. Pan, H. Gebru, X. Wang, J. Liu, J. Liu, Z. Li, K. Guo, *J. Mater. Chem. B* **2017**, *5*, 679.
[85] C. Fetsch, J. Gaitzsch, L. Messager, G. Battaglia, R. Luxenhofer, *Sci. Rep.* **2016**, *6*, 33491.
[86] E. Ostuni, R. G. Chapman, R. E. Holmlin, S. Takayama, G. M. Whitesides, *Langmuir* **2001**, *17*, 5605.
[87] B. Weber, A. Birke, K. Fischer, M. Schmidt, M. Barz, *Macromolecules* **2018**, *51*, 2653.
[88] R. Luxenhofer, C. Fetsch, A. Grossmann, *J. Polym. Sci., Part A: Polym. Chem.* **2013**, *51*, 2731.
[89] N. Gangloff, J. Ulbricht, T. Lorson, H. Schlaad, R. Luxenhofer, *Chem. Rev.* **2016**, *116*, 1753.
[90] O. Schäfer, D. Huesmann, M. Barz, *Macromolecules* **2016**, *49*, 8146.
[91] C. Fetsch, A. Grossmann, L. Holz, J. F. Nawroth, R. Luxenhofer, *Macromolecules* **2011**, *44*, 6746.
[92] H. R. Kricheldorf, *α-Aminoacid-N-Carboxy-Anhydrides and Related Heterocycles: Syntheses, Properties, Peptide Synthesis, Polymerization*, 1st ed., Springer, Berlin **1987**.
[93] W. Zhao, Y. Gnanou, N. Hadjichristidis, *Polym. Chem.* **2015**, *6*, 6193.
[94] B. A. Chan, S. Xuan, M. Horton, D. Zhang, *Macromolecules* **2016**, *49*, 2002.
[95] S. Gradisar, E. Zagar, D. Pahovnik, *ACS Macro Lett.* **2017**, *6*, 637.
[96] X. Zhang, S. Monge, M. In, O. Giani, J.-J. Robin, *Soft Matter* **2013**, *9*, 1301.
[97] T. Stukenkemper, J. Jansen, C. Lavilla, A. Dias, D. Brougham, A. Heise, *Polym. Chem.* **2017**, *8*, 828.
[98] H. Peng, J. Ling, Y. Zhu, L. You, Z. Shen, *J. Polym. Sci., Part A: Polym. Chem.* **2012**, *50*, 3016.
[99] J. Ling, H. Peng, Z. Shen, *J. Polym. Sci., Part A: Polym. Chem.* **2012**, *50*, 3743.
[100] T. Bai, J. Ling, *J. Phys. Chem. A* **2017**, *121*, 4588.
[101] X. Tao, M.-H. Li, J. Ling, *Eur. Polym. J.* **2018**, *109*, 26.
[102] X. Tao, Y. Deng, Z. Shen, J. Ling, *Macromolecules* **2014**, *47*, 6173.
[103] X. Tao, B. Zheng, T. Bai, M.-H. Li, J. Ling, *Macromolecules* **2018**, *51*, 4494.
[104] K. Johann, D. Svatunek, C. Seidl, S. Rizzelli, T. A. Bauer, L. Braun, K. Koynov, H. Mikula, M. Barz, *Polym. Chem.* **2020**, *11*, 4396.
[105] R. Kakuchi, P. Theato, *Functional Polymers by Post-Polymerization Modification: Concept, Guidelines, and Application*, 1st ed., Wiley-VCH Verlag GmbH & Co. KGaA **2013** (pp. 45–64).
[106] U. S. Gunay, B. Ozsoy, H. Durmaz, G. Hizal, U. Tunca, *J. Polym. Sci., Part A: Polym. Chem.* **2013**, *51*, 4667.
[107] D. J. Hall, H. M. Van Den Berghe, A. P. Dove, *Polym. Int.* **2011**, *60*, 1149.
[108] S. I. Subnaik, C. E. Hobbs, *Polym. Chem.* **2019**, *10*, 4524.
[109] C. Barner-Kowollik, F. E. Du Prez, P. Espeel, C. J. Hawker, T. Junkers, H. Schlaad, W. Van Camp, *Angew. Chem., Int. Ed.* **2011**, *50*, 60.
[110] R. Luxenhofer, *Z. Naturforsch., C: J. Biosci.* **2020**, *75*, 303.
[111] H. Jatzkewitz, *Z. Physiol. Chem.* **1954**, *297*, 149.
[112] H. Jatzkewitz, *Z. Naturforsch., B* **1955**, *10*, 27.
[113] P. Ferruti, A. Bettelli, A. Fere, *Polymer* **1972**, *13*, 462.
[114] H. G. Batz, G. Franzmann, H. Ringsdorf, *Macromol. Chem. Phys.* **1973**, *172*, 27.
[115] A. Das, P. Theato, *Chem. Rev.* **2016**, *116*, 1434.
[116] H. C. Kolb, K. B. Sharpless, *Drug Discovery Today* **2003**, *8*, 1128.
[117] D. J. V. van Steenis, O. R. David, G. P. van Strijdonck, J. H. van Maarseveen, J. N. Reek, *Chem. Commun.* **2005**, 4333.
[118] R. A. Evans, *Aust. J. Chem.* **2007**, *60*, 384.
[119] P. K. Avti, D. Maysinger, A. Kakkar, *Molecules* **2013**, *18*, 9531.
[120] J. Huo, C. Lin, J. Liang, *React. Funct. Polym.* **2020**, *152*, 104531.
[121] J.-F. Lutz, Z. Zarafshani, *Adv. Drug Delivery Rev.* **2008**, *60*, 958.
[122] O. Schäfer, M. Barz, *Chem.–Eur. J.* **2018**, *24*, 12131.
[123] W. Zhang, K. Chen, G. Chen, in *Click Reactions in Organic Synthesis* (Ed: S. Chandrasekaran), Wiley-VCH Verlag GmbH & Co. KGaA, Weinheim **2016**.
[124] B. Huang, X. Liu, L. Tan, Z. Cui, X. Yang, D. Jing, D. Zheng, Z. Li, Y. Liang, S. Zhu, *Biomater. Sci.* **2019**, *7*, 5383.
[125] J. Zhang, Y. Chen, M. A. Brook, *Langmuir* **2013**, *29*, 12432.
[126] O. Schäfer, K. Klinker, L. Braun, D. Huesmann, J. Schultze, K. Koynov, M. Barz, *ACS Macro Lett.* **2017**, *6*, 1140.
[127] J. C. Lim, J. M. Gruschus, G. Kim, B. S. Berlett, N. Tjandra, R. L. Levine, *J. Biol. Chem.* **2012**, *287*, 25596.
[128] D. H. Bianchi, *Biomed. Health Sci. Res.* **2014**, *2*, 222.
[129] B. Sun, C. Luo, H. Yu, X. Zhang, Q. Chen, W. Yang, M. Wang, Q. Kan, H. Zhang, Y. Wang, *Nano Lett.* **2018**, *18*, 3643.
[130] J. R. Winther, C. Thorpe, *Biochim. Biophys. Acta* **2014**, *1840*, 838.
[131] G. Ferrer-Sueta, B. Manta, H. Botti, R. Radi, M. Trujillo, A. Denicola, *Chem. Res. Toxicol.* **2011**, *24*, 434.
[132] D. Sheehan, B. McDonagh, J. A. Bárcena, *Expert Rev. Proteom.* **2010**, *7*, 1.
[133] R. M. Strongin, L. Hakuna, H. Peng, W. Chen, Y. Cheng, B. Wang, *Sensors* **2012**, *12*, 15907.
[134] J. Sun, H. Schlaad, *Macromolecules* **2010**, *43*, 4445.
[135] P. Ochtrop, C. P. R. Hackenberger, *Curr. Opin. Chem. Biol.* **2020**, *58*, 28.
[136] J.-S. Zheng, S. Tang, Y.-C. Huang, L. Liu, *Acc. Chem. Res.* **2013**, *46*, 2475.
[137] P. A. Jackson, J. C. Widen, D. A. Harki, K. M. Brummond, *J. Med. Chem.* **2017**, *60*, 839.
[138] A. Stanic, S. Uhlig, A. Solhaug, F. Rise, A. L. Wilkins, C. O. Miles, *J. Agric. Food Chem.* **2015**, *63*, 7556.
[139] D. Sticker, R. Geczy, U. O. Häfeli, J. P. Kutter, *ACS Appl. Mater. Interfaces* **2020**, *12*, 10080.
[140] B. J. Johnson, P. M. Jacobs, *Chem. Commun.* **1968**, 73b.
[141] B. J. Johnson, T. A. Ruettinger, *J. Org. Chem.* **1970**, *35*, 255.
[142] B. J. Johnson, D. S. Rea, *Can. J. Chem.* **1970**, *48*, 2509.
[143] W.-Y. Chen, M.-L. Hsu, R. K. Olsen, *J. Org. Chem.* **1975**, *40*, 3110.
[144] L. M. Siemens, F. W. Rottnek, L. S. Trzupek, *J. Org. Chem.* **1990**, *55*, 3507.
[145] S.-Y. Cho, B.-D. Park, S.-M. Oh, Y.-S. Lee, *Bull. Korean Chem. Soc.* **1994**, *15*, 324.
[146] S. Popovic, H. Bieräugel, R. J. Detz, A. M. Kluwer, J. A. Koole, D. E. Streefkerk, H. Hiemstra, J. H. van Maarseveen, *Chem.–Eur. J.* **2013**, *19*, 16934.
[147] A. Doriti, S. M. Brosnan, S. M. Weidner, H. Schlaad, *Polym. Chem.* **2016**, *7*, 3067.
[148] S. Yamada, K. Koga, T. Endo, *J. Polym. Sci., Part A: Polym. Chem.* **2012**, *50*, 2527.
[149] F. Fuchs, *Ber. Dtsch. Chem. Ges.* **1922**, *55*, 2943.
[150] H. Gebru, X. Wang, Z. Li, J. Liu, J. Xu, H. Wang, S. Xu, F. Wei, H. Zhu, K. Guo, *Pure Appl. Chem.* **2019**, *91*, 363.
[151] Ö. Alver, C. Parlak, M. Bilge, *Bull. Chem. Soc. Ethiop.* **2011**, *25*, 437.

[152] A. M. Rydzik, I. K. Leung, G. T. Kochan, M. A. McDonough, T. D. Claridge, C. J. Schofield, *Angew. Chem.* **2014**, *126*, 11105.
[153] B. J. Johnson, E. G. Trask, *J. Org. Chem.* **1968**, *33*, 4521.
[154] B. J. Johnson, P. M. Jacobs, *J. Org. Chem.* **1968**, *33*, 4524.
[155] J. Ulbricht, *Insights into Polymer Biodegradation – Investigations on Oxidative, Hydrolitic and Enzymatic Pathways*, Julius-Maximilians University Würzburg, Würzburg **2017**.
[156] Y.-C. M. Wu, T. M. Swager, *J. Am. Chem. Soc.* **2019**, *141*, 12498.
[157] R. Zhang, W. Wu, *J. Mol. Liq.* **2011**, *162*, 20.
[158] A. Tsutsui, Y. Morishita, H. Furumachi, T. Fujimoto, R. Hirai, T. Fujita, T. Machinami, *Tetrahedron Lett.* **2021**, *68*, 152836.
[159] K. Mitamura, N. Hori, S. Mino, T. Iida, A. F. Hofmann, S. Ikegawa, *Chem. Phys. Lipids* **2012**, *165*, 261.
[160] M. Glassner, S. Maji, R. Victor, N. Vanparijs, K. Ryskulova, B. G. De Geest, R. Hoogenboom, *Polym. Chem.* **2015**, *6*, 8354.
[161] G. G. Alvaradejo, M. Glassner, R. Hoogenboom, G. Delaittre, *RSC Adv.* **2018**, *8*, 9471.
[162] T. X. Viegas, M. D. Bentley, J. M. Harris, Z. Fang, K. Yoon, B. Dizman, R. Weimer, A. Mero, G. Pasut, F. M. Veronese, *Bioconjugate Chem.* **2011**, *22*, 976.
[163] F. M. Veronese, *Biomaterials* **2001**, *22*, 405.
[164] D. Bontempo, K. L. Heredia, B. A. Fish, H. D. Maynard, *J. Am. Chem. Soc.* **2004**, *126*, 15372.
[165] B. Jung, P. Theato, in *Bio-Synthetic Polymer Conjugates. Advances in Polymer Science* (Ed: H. Schlaad), Springer, Berlin **2012**, pp. 37–70.

